



Original articles

Research article

<https://doi.org/10.17308/kcmf.2026.28/13563>Stability against crystallization and optical properties of $(\text{Ga}_{10}\text{Ge}_{15}\text{Te}_{75})_{100-x}(\text{AgI})_x$ ($x = 0\text{--}15$ mol %) glassesE. A. Tyurina¹, A. P. Velmuzhov¹✉, M. V. Sukhanov¹, A. D. Plekhovich¹, D. G. Fukina², V. S. Shiryaev¹¹G. G. Devyatykh Institute of Chemistry of High-Purity Substances of the Russian Academy of Sciences, 49, Tropinin st., Nizhny Novgorod 603951, Russian Federation²Lobachevsky State University of Nizhny Novgorod, 23, Gagarin aven., Nizhny Novgorod 603950, Russian Federation

Abstract

Objectives: Germanium telluride based glasses, due to their wide transparency range and high refractive index, are promising optical materials for the middle infrared range. The tendency of such glasses to crystallize, which limits their practical application, requires the search for new compositions and the study of their properties. The aim of this work was to investigate the stability against crystallization and optical transparency of $(\text{Ga}_{10}\text{Ge}_{15}\text{Te}_{75})_{100-x}(\text{AgI})_x$ ($x = 0\text{--}15$ mol %) glasses as new materials for fiber optics.

Experimental: The glasses were analyzed using differential scanning calorimetry, scanning electron microscopy combined with X-ray spectral microanalysis, and near- and mid-infrared spectroscopy. The main goal of the work is the establishment of high stability against crystallization of the studied glasses with a silver iodide content of 5–15 mol %.

Conclusions: This makes it possible to consider such glasses as one of the most promising materials for the production of fibers with low optical losses in the spectral range of 4–15 μm .

Keywords: Chalcogenide glass, Germanium telluride, Silver iodide, Crystallization, Middle infrared materials, Optical transmittance

Funding: The work was financially supported by the Russian Science Foundation (Project No. 25-13-20046, Russia), <https://rscf.ru/project/25-13-20046/>.

For citation: Tyurina E. A., Velmuzhov A. P., Sukhanov M. V., Plekhovich A. D., Fukina D. G. Stability against crystallization and optical properties of $(\text{Ga}_{10}\text{Ge}_{15}\text{Te}_{75})_{100-x}(\text{AgI})_x$ ($x = 0\text{--}15$ mol %) glasses. *Condensed Matter and Interphases*. 2026;28(1): 115–125. <https://doi.org/10.17308/kcmf.2026.28/13563>

Для цитирования: Тюрина Е. А., Вельмузов А. П., Суханов М. В., Плехович А. Д., Фукина Д. Г. Кристаллизационная устойчивость и оптические свойства стекол системы $(\text{Ga}_{10}\text{Ge}_{15}\text{Te}_{75})_{100-x}(\text{AgI})_x$ ($x = 0\text{--}15$ мол. %). *Конденсированные среды и межфазные границы*. 2026;28(1): 115–125. <https://doi.org/10.17308/kcmf.2026.28/13563>

✉ Aleksandr P. Velmuzhov, e-mail: velmuzhov.ichps@mail.ru

© Tyurina E. A., Velmuzhov A. P., Sukhanov M. V., Plekhovich A. D., Fukina D. G., 2026



The content is available under Creative Commons Attribution 4.0 License.

1. Introduction

Glasses based on the Ge – Te system are among the most promising optical materials for the middle infrared (mid-IR) range [1]. They have a wide transparency window extending from 2 to 30 μm (some compositions up to 35 μm [2]) and high refractive index values [3]. Optical fibers made of glasses based on the Ge–Te system are transparent up to 16 μm [4]. Therefore, these materials are used for the production of fiber-optic sensors [4, 5], transmission of CO_2 laser radiation with operating wavelengths of 9.3 and 10.6 μm [6], and for solving problems related to space exploration [7, 8].

The main disadvantage of glasses based on the Ge–Te binary system is a pronounced tendency to crystallization [9]. To increase their stability against crystallization, components promoting glass formation are added to their composition. The most suitable of these components is silver iodide. To date, glasses of the Ge – Te – AgI system are the only representatives of germanium telluride glassy materials that do not crystallize upon heating during analysis by differential scanning calorimetry at a heating rate of 10 K/min [10, 11]. The crystallization stability of these materials allows them to be used to manufacture optical fibers. However, optical losses in these fibers are high compared to Ge–S and Ge–Se systems [12]. One of the main reasons for this is partial crystallization of samples during fiber drawing [4]. Recently, the authors of the work fabricated a $(\text{Ge}_{21}\text{Te}_{79})_{50}(\text{AgI})_{50}$ glass fiber with optical losses of less than 1 dB/m in the spectral range of 7.2–10.9 μm , which is a record among telluride systems [13]. One of the key areas for further reduction of optical losses in germanium telluride fibers is optimization of the chemical composition of the glass. In this regard, the study of novel glasses based on the Ge–Te–AgI system is an actual scientific task.

The aim of this work was to investigate the stability against crystallization and optical transparency of glasses of the $(\text{Ga}_{10}\text{Ge}_{15}\text{Te}_{75})_{100-x}(\text{AgI})_x$ ($x = 0–15$ mol %) system as new materials for fiber optics. The choice of the system was due to the higher glass-forming ability of Ga – Ge – Te glasses compared to binary Ge – Te compositions. Within the Ga – Ge – Te system, one of the most stable against crystallization is the $\text{Ga}_{10}\text{Ge}_{15}\text{Te}_{75}$

composition [14], which was chosen as the base variant. There is only one publication in the literature on the study of the properties of glasses of the $(\text{Ga}_{10}\text{Ge}_{15}\text{Te}_{75})_{100-x}(\text{AgI})_x$ system, the results of which indicate an unexpectedly low stability against crystallization [15], which, in the authors' opinion, requires clarification.

2. Experimental

2.1. Glass preparation

To avoid any misunderstandings in the chemical composition of telluride glasses containing silver iodide, available in the literature (e.g., [2] and [16]), the equations used to specify the component ratios are given below:

$$y(\text{Ga}) = 0.1 \times (100 - 2x), \quad (1)$$

$$y(\text{Ge}) = 0.15 \times (100 - 2x), \quad (2)$$

$$y(\text{Te}) = 0.75 \times (100 - 2x), \quad (3)$$

$$y(\text{Ag}) = n(\text{I}) = x, \quad (4)$$

where $y(\dots)$ is the component concentration, at. %; x is the variable in the formula $(\text{Ga}_{10}\text{Ge}_{15}\text{Te}_{75})_{100-x}(\text{AgI})_x$.

To prepare the glass, 6N gallium (JSC “Lankhit”, Moscow, Russia), 5N germanium (JSC “Germanium”, Krasnoyarsk, Russia), and 5N tellurium (JSC “ADV-Engineering”, Zelenograd, Russia) were used. Silver iodide was prepared by passing 3N iodine (JSC “Khimreaktiv”, Russia) over metallic silver (JSC “Novosibirsk Rare Metals Plant”, Russia) in a vacuum silica-glass reactor. The iodine was preliminarily triple sublimated to remove metal impurities and water.

The $(\text{Ga}_{10}\text{Ge}_{15}\text{Te}_{75})_{100-x}(\text{AgI})_x$ glasses were prepared by melting the batch in silica-glass glass ampoules with an internal diameter of 7 mm and a wall thickness of 1.5 mm. The ampoules were pre-washed with a mixture of hydrofluoric, hydrochloric, and nitric acids, deionized water, then dried and baked in a flow of especially pure oxygen at 980 °C to remove OH groups [17]. The batch was evacuated to a residual pressure of no more than 10^{-3} Pa, the ampoules were sealed-off. The homogenization of the glass-forming melt was carried out in a rocking muffle furnace at a temperature of 750–850 °C, depending on the glass composition, for 6 hours. The melt was quenched by quickly immersing the ampoules in

water. To relieve mechanical stress, the glasses were annealed at 150–170 °C for 30 minutes, with subsequent cooling to room temperature in the furnace off mode. To extract the samples, the ampoules were cut with a diamond disk. The resulting glass samples had compositions of $(\text{Ga}_{10}\text{Ge}_{15}\text{Te}_{75})_{100-x}(\text{AgI})_x$ ($x = 0, 3, 5, 8, 10, 12, 15$) in the form of cylindrical rods up to 100 mm long. For brevity, the samples were designated as GGTAI- x .

2.2. Differential scanning calorimetry

The samples were investigated by means of differential scanning calorimetry (DSC) using an STA 409 PC Luxx microcalorimeter (Netzsch, Germany) in a high-purity argon flow in the temperature range of 50–450 °C at a heating rate of 10 deg/min. The measurements were carried out in aluminum pans, the mass of the samples in the form of irregularly shaped pieces was ≈ 30 mg. Preliminary calibration of the device using standard samples ensured a temperature measurement accuracy of ± 0.1 °C. The error in determining the glass transition temperature (T_g), the onset of crystallization (T_x), and the onset of crystal melting (T_m) was ± 2 °C; the error in determining the temperature of maximum crystallization (T_p) was ± 1 °C. The generally accepted criterion $\Delta T = T_x - T_g$ [18] was used as a parameter characterizing the glass stability against crystallization. According to established practice, glasses with a ΔT value > 120 °C are suitable for drawing optical fibers [19].

To increase the reliability of the DSC analysis results, as one of the key analytical methods in this study, repeated measurements were performed on additionally synthesized glass samples. Glass with the $(\text{Ga}_{10}\text{Ge}_{15}\text{Te}_{75})_{92}(\text{AgI})_8$ composition was additionally studied at heating rates of 2.5 and 5 K/min.

2.3. Scanning electron microscopy

The stability against crystallization of the glasses was additionally studied by means of scanning electron microscopy (SEM). The analysis was performed using a JSM-IT300LV electron microscope (JEOL) with backscattered and secondary electrons. The elemental composition of the surfaces was measured by means of energy-dispersive X-ray microanalysis (EDXMA) using an attachment with an X-MaxN 20 detector (Oxford

Instruments). For the study, disc-shaped samples with parallel-plane polished faces were used. The samples were pre-annealed for 1 hour in evacuated silica-glass ampoules at a temperature of $T_g + 120$ °C, corresponding to the conditions for drawing fiber. After annealing, the samples were re-polished to remove vapor condensation products from their surfaces.

2.4. IR spectroscopy

The transparency of the glasses in the spectral range of 2–25 μm was studied using a Fourier-transform IR Tensor 27 spectrometer (Bruker, Germany) at a resolution of 4 cm^{-1} . The samples used for the measurements were 2-mm-thick disks with parallel-plane polished edges. Based on the obtained data, absorption coefficient spectra $\alpha(\lambda)$ were plotted:

$$\alpha(\lambda) = -\frac{\ln(T(\lambda))}{l}, \quad (5)$$

where $T(\lambda)$ is the transparency; l is the sample thickness (cm).

To clarify the position of the short-wavelength transparency edge of the glasses, additional measurements were carried out in the spectral region of 1–3 μm using a UV 3600 spectrophotometer (Shimadzu, Japan) at a resolution of 2 nm. The energy of direct optical transitions and the corresponding short-wavelength transparency edge were determined using the generally accepted method for chalcogenide glasses in coordinates $(\alpha h\nu)^{1/2} = f(h\nu)$, where α is the absorption coefficient, h is Planck's constant, and ν is the radiation frequency [20].

3. Results and discussion

3.1. Stability against crystallization

The DSC heating curves of the prepared samples are shown in Fig. 1a. The curves exhibit devitrification ranges typical for glasses. For samples GGTAI-0 and GGTAI-3, an exothermic peak of glass crystallization and an endothermic peak of crystal melting are observed. The curve for sample GGTAI-5 shows weak endothermic signals in the 320–340 °C range, the nature of which requires clarification (melting of a small amount of the crystalline phase or fluctuations associated, for example, with the non-stationarity of the inert

gas flow). The characteristic temperature values of the samples are given in Table 1. The glass transition temperature decreases monotonically with an increase in the silver iodide content (Fig. 1b). From the standpoint of the structural approach, this is due to a decrease in the overall connectivity of the glass network due to the “loosening” effect of iodine, and an increase in the ionic nature of chemical bonds [21, 22]. Fig. 1b (curve 2) shows the dependence of T_g on the average coordination of atoms in glass $\langle r \rangle$, calculated using the equation:

$$\langle r \rangle = \sum r_i x_i, \quad (6)$$

where r_i is the coordination number of the i -th atom; x_i is the atomic fraction [23]. In accordance with the literature data for chalcogenide glasses, it was assumed that $r_{\text{Ge}} = 4$, $r_{\text{Ga}} = 4$, $r_{\text{Te}} = 2$, $r_{\text{Ag}} = 3$; $r_{\text{I}} = 1$ [24–27]. The obtained dependence fits the general trend for glassy materials of decreasing T_g with a decreasing average coordination number [28].

According to the obtained results, glasses with a silver iodide content of 5–15 mol % do not

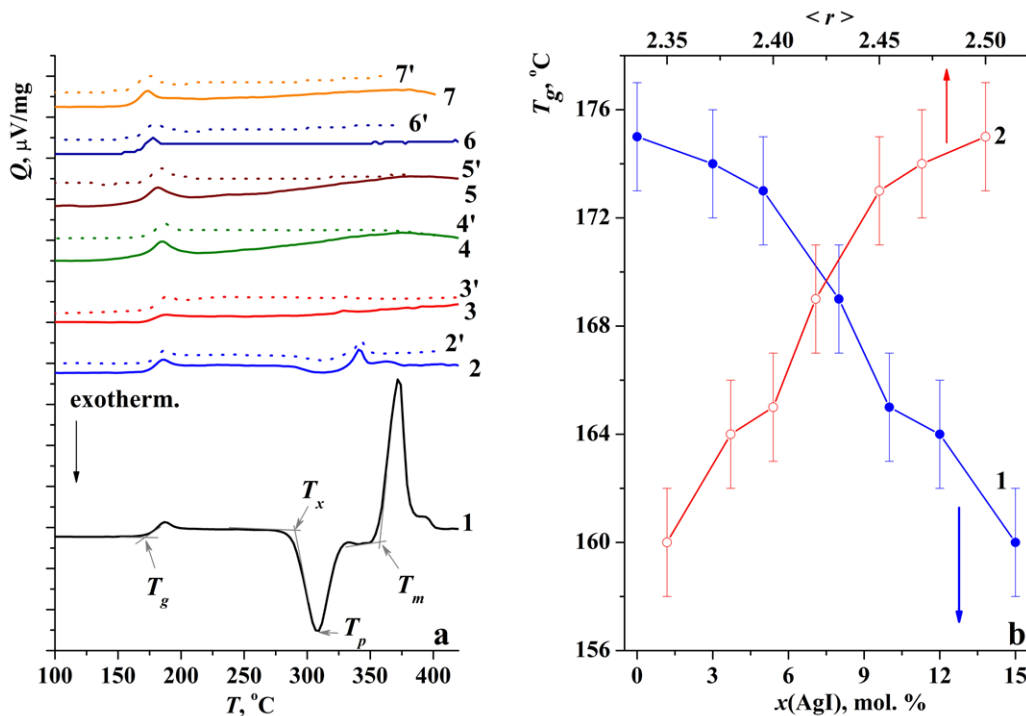


Fig. 1. The DSC heating curves of $(\text{Ga}_{10}\text{Ge}_{15}\text{Te}_{75})_{100-x}(\text{AgI})_x$ ($x = 0, 3, 5, 8, 10, 12, 15$) glasses based on the results of two independent experiments (a) and the influence of silver iodide content (1b) and average coordination of atoms (2b) on their glass transition temperature

Table 1. Characteristic temperatures, energy of direct optical transitions and position of the short-wavelength transparency edge of $(\text{Ga}_{10}\text{Ge}_{15}\text{Te}_{75})_{100-x}(\text{AgI})_x$ glasses

Sample	$T_g, \pm 2 \text{ }^\circ\text{C}$	$T_x, \pm 2 \text{ }^\circ\text{C}$	$\Delta T, \pm 2 \text{ }^\circ\text{C}$	$T_p, \pm 1 \text{ }^\circ\text{C}$	$T_m, \pm 2 \text{ }^\circ\text{C}$	$E_g \pm 0.01 \text{ eV}$	$\lambda_{\text{cut.}}, \pm 2 \text{ nm}$
GGTAI-0	175	289	114	308	357	0.59	2116
GGTAI-3	174	290	116	312	339	0.63	1981
GGTAI-5	173	–	–	–	–	0.64	1925
GGTAI-8	169	–	–	–	–	0.65	1899
GGTAI-10	165	–	–	–	–	0.66	1884
GGTAI-12	164	–	–	–	–	0.67	1840
GGTAI-15	160	–	–	–	–	0.70	1771

crystallize during DSC analysis at a heating rate of 10 K/min. This refutes the previously presented data on the crystallization stability of glasses of the $(\text{Ga}_{10}\text{Ge}_{15}\text{Te}_{75})_{100-x}(\text{AgI})_x$ system [15]. The authors of that work reported crystallization of glasses upon heating to 259–266 °C. Moreover, the disappearance of the exothermic peak of crystallization in the studied system occurs at lower concentrations of silver iodide compared to the $(\text{GeTe}_4)_{100-x}(\text{AgI})_x$ system [10]. This is due to the increased crystallization stability of the $\text{Ga}_{10}\text{Ge}_{15}\text{Te}_{75}$ base glass.

To further confirm the stability of the studied glasses against crystallization, Fig. 2 shows the DSC curves of the GGTAI-8 sample at lower heating rates: 5 and 2.5 K/min. The choice of the composition for the study is due to the fact that for practical applications it is desirable that crystallization stability be achieved with the minimum possible content of silver iodide. This is due to the low chemical stability of chalcogenide glasses with high iodine content. A decrease in the thermal scanning rate does not lead to the appearance of an exothermic crystallization peak, which indicates a high glass-forming ability of the sample. From the obtained data, the enthalpy of glass transition activation [29] was calculated using the equation:

$$\frac{d \ln V}{dT_g} = \frac{\Delta h^*}{R}, \quad (7)$$

where V is the heating rate, K/min; R is the universal gas constant, J/(mol·K). The obtained value was 320 ± 25 kJ/mol. This parameter does not provide direct information on the crystallization stability of glasses. However, it was found that is close in value to the enthalpy of activation of viscous flow [30], which is used to calculate relaxation processes in glasses and evaluate the kinetic criteria of glass formation.

Fig. 3 shows SEM images of the surface of samples GGTAI-3 and GGTAI-12 after annealing at a temperature of $T_g + 120$ °C. Low contrast due to the small size and concentration of crystals prevented the detection of clusters of crystalline inclusions on the polished surface. Clear images of the crystalline phase were captured in pores measuring 100–300 μm , formed due to partial evaporation of volatile glass components. Such pores can act as crystallization centers for the glass. All pores in sample GGTAI-3 contained a high concentration of crystals (estimated, > 30 vol. %) with an average size of 2 μm . In samples with a silver iodide content of 5–15 mol %, crystalline inclusions were captured in individual large pores, and their proportion did

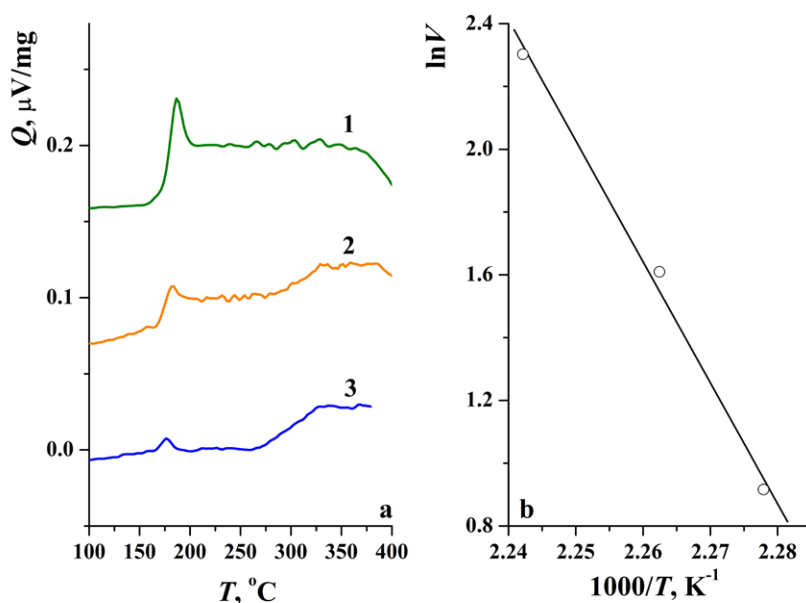


Fig. 2. DSC heating curves of the GGTAI-8 sample at heating rates of 10 K/min (1a), 5 K/min (2a) and 2.5 K/min (3a) and linearization of the $\ln V$ dependence on $1/T_g$ to determine the enthalpy of glass transition activation (b)

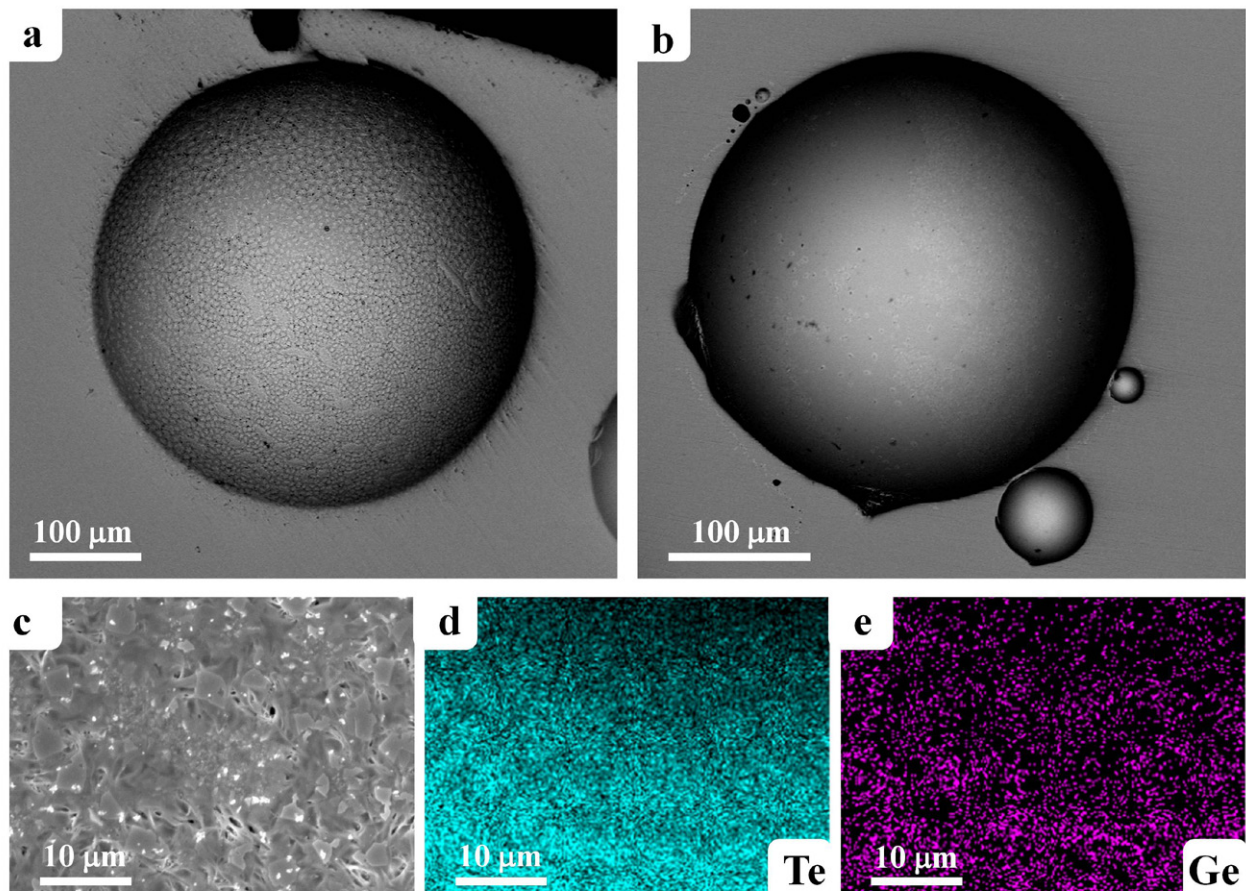


Fig. 3. Electronic images of the surface of the GGTAI-3 and GGTAI-12 samples after annealing at $T_g + 120$ °C for an hour; a – pore in the GGTAI-3 sample; b – pore in the GGTAI-12 sample; c – image of crystals inside the pores of the GGTAI-3 sample; d, e – corresponding this image shows the distribution maps of Te and Ge

not exceed 10 % of the pore volume. According to the element distribution maps over the surface of the samples, the forming crystalline phase corresponds to tellurium. This is consistent with known literature data on the crystallization of telluride glasses [14, 16]. The total volume fraction of crystalline inclusions in the annealed samples did not exceed 1 vol. % (the detection limit of the crystalline phase in the glass matrix for X-ray phase analysis under the used imaging conditions). In reality, when drawing fiber from a rod [4], the time the sample is kept at the maximum process temperature does not exceed 5 min. This suggests that, under actual drawing conditions, GGTAI-5–GGTAI-15 glasses will not undergo crystallization.

The observed high stability against crystallization of the $(\text{Ga}_{10}\text{Ge}_{15}\text{Te}_{75})_{100-x}(\text{AgI})_x$ ($x = 5\text{--}15$ mol %) glasses may be due to several factors, including various approaches to glass formation. Some of these are listed below:

- approaching the optimal average coordination of atoms with an increase in the proportion of silver iodide, which, according to the topological Phillips criterion [23], for glasses with a three-dimensional structural network corresponds to a value of 2.4. This criterion, however, does not explain the difference between the glass-forming ability of the Ge – Te – AgI and Ga – Ge – Te – AgI systems due to the close values of the coordination numbers of germanium and gallium in chalcogenide glasses;

- complication of the glass network structure due to the formation of structural fragments of the $[\text{MeTe}_{(4-x)/2}]_x$ type, where Me = Ge, Ga; $x = 0\text{--}4$ [24, 25, 31]. This explains the increase in the glass-forming ability of germanium telluride glasses with the addition of gallium, associated with the appearance of new $[\text{GaTe}_{(4-x)/2}]_x$ structural units;

- a decrease in the liquidus temperature (or glass transition) in the $(\text{Ga}_{10}\text{Ge}_{15}\text{Te}_{75})_{100-x}(\text{AgI})_x$

system with an increase in the proportion of AgI while maintaining a relatively high average bond energy, corresponding to the modified San-Rawson criterion [28]. This criterion is mainly fulfilled due to the formation of strong Ga–I chemical bonds during structural transformations of the type



The corresponding bond energies have the following values (in kJ/mol): $E_{\text{Ga-I}} = 339$; $E_{\text{Ga-Te}} = 265$; $E_{\text{Ag-I}} = 252$; $E_{\text{Ag-Te}} = 196$ [32]. The formation of the silver telluride phase during the distillation of Ge–Te–AgI glasses, confirming the possible occurrence of the indicated process, was reported earlier in [33].

The presented arguments do not claim to strictly substantiate the glass-forming ability of the $(\text{Ga}_{10}\text{Ge}_{15}\text{Te}_{75})_{100-x}(\text{AgI})_x$ system, but they indicate the naturally expected high stability of glasses against crystallization, which was confirmed experimentally in this work.

3.2. Optical transparency

The absorption spectra of the prepared glasses in the spectral range of 2–25 μm are shown in Fig. 4a. The spectra exhibit intense absorption bands in the range of 15–20 μm , corresponding

to the gallium oxide impurity. This impurity is present in the initial gallium and additionally appears during the glass synthesis process due to the reduction of germanium and tellurium oxides due to the high thermodynamic stability of Ga_2O_3 ($\Delta_f G^0(298.15) = -998.339$ [34]). This explains the low (below the detection limit) intensity of the absorption bands from the impurities of the oxides of the remaining glass components. There is no generally accepted criterion in the literature for assessing the long-wavelength transparency edge of chalcogenide glasses. In this work, the absorption coefficient value at a wavelength of 23 μm was used as such a comparative characteristic, since the maximum of the intrinsic absorption band of the glass matrix, which limits the transparency of optical fibers, is located in this region. Fig. 4b shows the obtained dependence of α on the silver iodide content. An increase in the proportion of AgI in the glasses leads to a decrease in the intensity of this absorption band. As was shown in [2] from a comparison of the transmission spectra of glasses of the $(\text{GeTe}_4)_{100-x}(\text{AgI})_x$ and $(\text{GeTe}_4)_{100-x}\text{Ag}_x$ systems, the observed broadening of the transparency window is due to the influence of iodine. In the harmonic approximation, the vibration frequency of atoms is proportional to the square root of

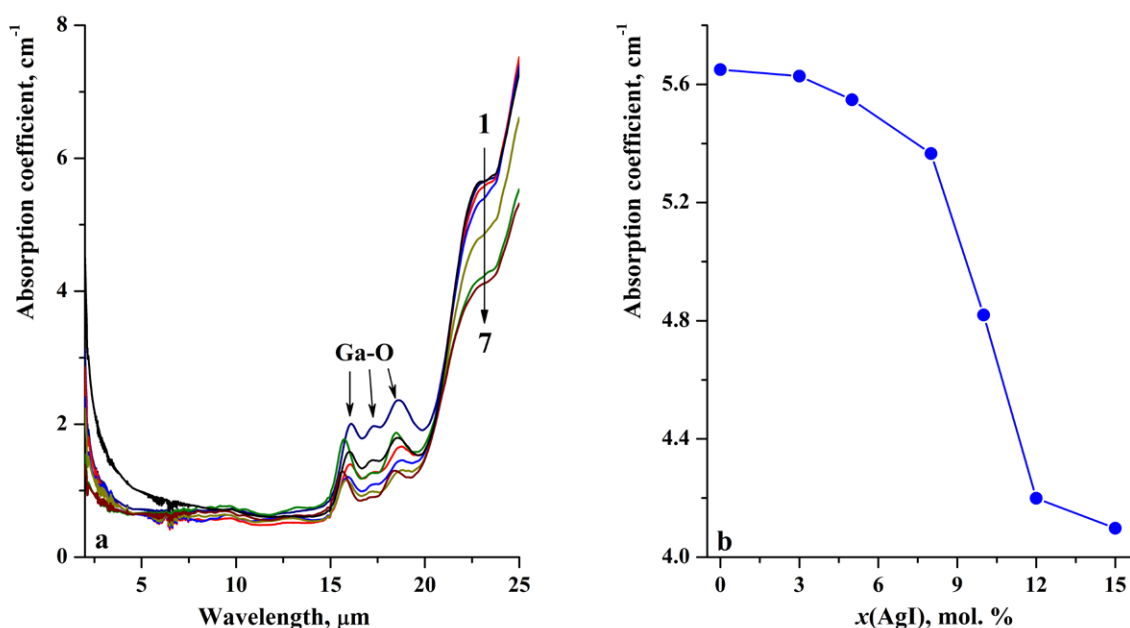


Fig. 4. Absorption spectra of the $(\text{Ga}_{10}\text{Ge}_{15}\text{Te}_{75})_{100-x}(\text{AgI})_x$ glass system in the range of 2–25 microns (a) and the dependence of the absorption coefficient at a wavelength of 23 microns on the glass composition (b). 1a: $x = 0$; 2a: $x = 3$; 3a: $x = 5$; 4a: $x = 8$; 5a: $x = 10$; 6a: $x = 12$; 7a: $x = 15$. The thickness of the samples is 2 mm

the ratio of the force constant of the bond to the reduced mass [35]. Since the atomic mass of I (126.90447(3) a.m.u.) is less than that of Te (127.60(3) a.m.u.) [36], the observed effect is due to the destructive action of iodine on the structural network, i.e., a decrease in the force constant. The sharp change in absorption in the range of silver iodide content of 8–12 mol % could be caused by the structural rearrangement of the glass network from three-dimensional to layered and pseudo-chain, described, for example, in [37] for the Ge–Se–I system. This effect also manifests itself in the dependence of T_g on the composition of the glasses (Fig. 1b).

The near-IR transmission spectra of glasses, the calculated E_g values (Fig. 5), and the corresponding positions of the short-wavelength transparency edge λ_{cut} are shown in Fig. 6 and Table 1. An increase in the AgI content in glasses leads to an increase in E_g and a shift of λ_{cut} to the short-wavelength region. According to generally accepted concepts, the energy of direct optical transitions in chalcogenide glasses is determined by the band structure of the short-range order elements of the glass network [38]. Based on this, the observed changes are associated with higher E_g values for germanium and silver iodides

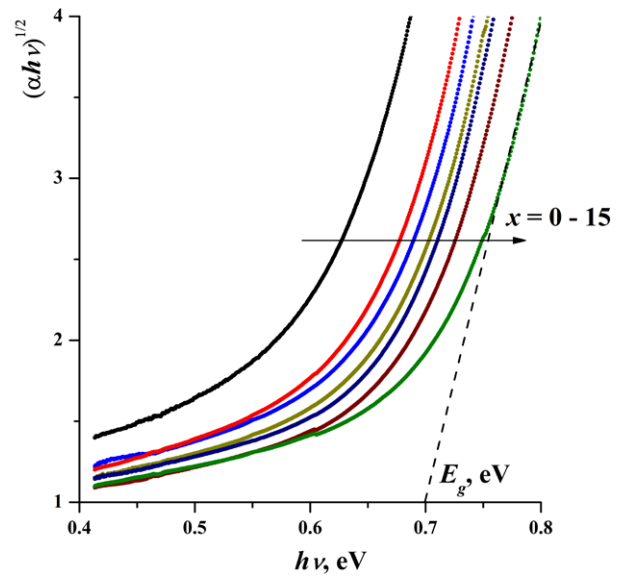


Fig. 5. Graphical determination of the direct optical transitions energy of $(\text{Ga}_{10}\text{Ge}_{15}\text{Te}_{75})_{100-x}(\text{AgI})_x$ ($x = 0, 3, 5, 8, 10, 12, 15$) chalcogenide glasses in coordinates $(\alpha hv)^{1/2} = f(hv)$

compared to germanium telluride: $E_g = 0.742$ eV for trigonal GeTe [39], 2.8 eV for GeI_2 [40], 2.37 eV for cubic AgI [41]. In addition, the position of the short-wavelength transparency edge and its absolute value can be affected by the phase homogeneity of the glass, which increases

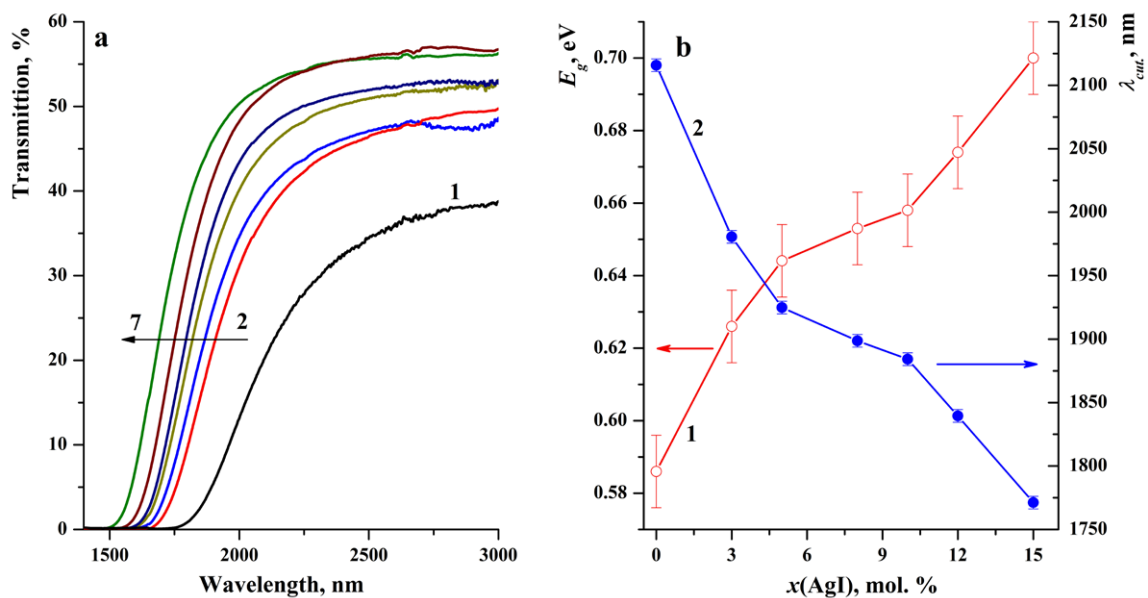


Fig. 6. Transmission spectra of the $(\text{Ga}_{10}\text{Ge}_{15}\text{Te}_{75})_{100-x}(\text{AgI})_x$ glass system in the range of 1–3 microns (a) and the dependence of E_g (1b) and λ_{cut} (2b) on the composition. 1a: $x = 0$; 2a: $x = 3$; 3a: $x = 5$; 4a: $x = 8$; 5a: $x = 10$; 6a: $x = 12$; 7a: $x = 15$. The thickness of the samples is 2 mm

with the addition of AgI due to the increased crystallization stability of the glasses. The most important positive result of shifting λ_{cut} to the short-wavelength region for glasses is the potentially more efficient pumping of rare earth elements in doped samples used as IR radiation sources [42]. For fiber sensor element materials, shifting the short-wavelength edge will improve the sensitivity to detecting substances absorbing in the 2–4 μm range (water, methane, etc.).

The results obtained indicate that the addition of silver iodide to $\text{Ga}_{10}\text{Ge}_{15}\text{Te}_{75}$ glass significantly improves its stability against crystallization and optical properties. This makes these materials promising competitors to Ge – Te – AgI glasses, which have been used to manufacture optical fibers with relatively low optical losses [4, 13]. Further research in this area could be aimed at optimizing the ratio of components of the base Ga – Ge – Te glass to more improve its stability against crystallization and at developing methods for producing Ga – Ge – Te – AgI glasses with extremely an low content of absorbing impurities.

4. Conclusions

Based on the results obtained in this work, the following key conclusions can be drawn:

- glasses of the $(\text{Ga}_{10}\text{Ge}_{15}\text{Te}_{75})_{100-x}(\text{AgI})_x$ system with a silver iodide content of 5–15 mol % are highly resistant to crystallization and do not show exothermic signals during DSC analysis at a heating rate of 10 K/min;

- increasing the silver iodide content in $(\text{Ga}_{10}\text{Ge}_{15}\text{Te}_{75})_{100-x}(\text{AgI})_x$ glasses increases their transparency in the long-wavelength region of the spectrum due to a decrease in the intensity of their intrinsic absorption bands;

- the fundamental absorption edge shifts to the short-wavelength region from 2116 ± 2 to 1771 ± 2 nm, as the proportion of AgI in these glasses increases from 0 to 15 mol %.

The obtained results makes it possible to consider glasses of the $(\text{Ga}_{10}\text{Ge}_{15}\text{Te}_{75})_{100-x}(\text{AgI})_x$ ($x = 5\text{--}15$ mol %) system as one of the most promising materials for the production of fibers with low optical losses in the spectral range of 4–16 μm .

Author contributions

E. A. Tyurina – Research concept, Methodology, Investigation, Original draft. A. P. Velmuzhov –

Research concept, Methodology, Investigation, Writing – review & editing. M. V. Sukhanov – Research concept, Methodology, Investigation, Writing – review & editing. A. D. Plekhovich – Methodology, Investigation, Writing – editing. D. G. Fukina – Methodology, Investigation, Writing – editing. V. S. Shiryaev – Research concept, Writing – review & editing.

Conflict of interests

The authors declare that they have no known competing financial interests or personal relationships that could have influenced the work reported in this paper.

References

1. Conseil C., Bastien J.-C., Boussard-Plédel C., ... Bureau B. Te-based chalcogenide glasses for far-infrared optical fiber. *Optical Materials Express*. 2012;2(11): 1470–1477. <https://doi.org/10.1364/OME.2.001470>
2. Le Coq D., Cui S., Boussard-Plédel C., ... Bureau B. Telluride glasses with far-infrared transmission up to 35 μm . *Optical Materials*. 2017;72: 809–812. <https://doi.org/10.1016/j.optmat.2017.07.038>
3. Gu J., Shen X., Jia G., Xia K. Optical properties of Ge-Ga-Ag-Te high refractive index chalcogenide glasses. *Optical Materials Express*. 2023;13(5): 1320–1327. <https://doi.org/10.1364/OME.484948>
4. Cui S., Boussard-Plédel C., Lucas J., Bureau B. Te-based glass fiber for far-infrared biochemical sensing up to 16 μm . *Optics Express*. 2014;22(18): 21253–21262. <https://doi.org/10.1364/OE.22.021253>
5. Shiryaev V. S., Velmuzhov A. P., Kotereva T. V., ... Karaksina E. V. Recent achievements in development of chalcogenide optical fibers for mid-IR sensing. *Fibers*. 2023;11: 54. <https://doi.org/10.3390/fib11060054>
6. Kotsuyama T., Matsumura H. Light transmission characteristics of telluridebased chalcogenide glass for infrared fiber application. *Journal of Applied Physics*. 1994;75: 2743. <https://doi.org/10.1063/1.356210>
7. Bureau B., Maurugeon S., Charpentier F., ... Zhang X.-H. Chalcogenide glass fibers for infrared sensing and space optics. *Fiber and Integrated Optics*. 2009;28: 65–80. <https://doi.org/10.1080/01468030802272542>
8. Zhang S., Zhang X., Barillot M., ... Parent G. Purification of $\text{Te}_{75}\text{Ga}_{10}\text{Ge}_{15}$ glass for far infrared transmitting optics for space application. *Optical Materials*. 2010;32: 1055–1059. <https://doi.org/10.1016/j.optmat.2010.02.030>
9. Savage J. A. Glass formation and D.S.C. data in the Ge-Te and As-Te memory glass systems. *Journal of Non-Crystalline Solids*. 1972;11(2): 121–130. [https://doi.org/10.1016/0022-3093\(72\)90294-3](https://doi.org/10.1016/0022-3093(72)90294-3)
10. Shiryaev V. S., Velmuzhov A. P., Churbanov M. F., ... Plotnichenko V. G. Preparation and investigation of high purity Ge-Te-AgI glasses for optical application. *Journal of Non-Crystalline Solids*. 2013;377: 1–7. <http://dx.doi.org/10.1016/j.jnoncrsol.2013.03.039>

11. Wang X., Nie Q., Wang G., ... Ma H., Investigations of Ge–Te–AgI chalcogenide glass for far-infrared application. *Spectrochimica Acta Part A: Molecular and Biomolecular Spectroscopy*. 2012;86: 586–589. <http://dx.doi.org/10.1016/j.saa.2011.11.018>
12. Lucas P., Boussard-Pledel C., Wilhelm A., ... Bureau B. The development of advanced optical fibers for long-wave infrared transmission. *Fibers*. 2013;1: 110–118. <https://doi.org/10.3390/fib1030110>
13. Velmuzhov A. P., Tyurina E. A., Sukhanov M. V., ... Shiryayev V. S. First <1dB/m optical loss fiber based on germanium telluride glasses. *Optics and Laser Technology*. 2025;192: 113727. <https://doi.org/10.1016/j.optlastec.2025.113727>
14. Upadhyay M., Murugavel S. Correlation between crystallization, electrical switching and local atomic structure of Ge–Te glasses. *Journal of Non-Crystalline Solids*. 2013;368: 34–39. <http://dx.doi.org/10.1016/j.jnoncrysol.2013.02.028>
15. Cheng C., Wang X., Xu T., ... Chen. W. Optical properties of Ag- and AgI-doped Ge–Ga–Te far-infrared chalcogenide glasses. *Infrared Physics & Technology*. 2016;76: 698–703. <https://doi.org/10.1016/j.infrared.2016.04.035>
16. Zhu E., Wu B., Zhao X., ... Tian P. Surface crystallization behavior and physical properties of $(\text{GeTe}_{85}\text{AgI}_{15})$ chalcogenide glass. *Infrared Physics & Technology*. 2017;86: 135–138. <https://doi.org/10.1016/j.infrared.2017.09.006>
17. Velmuzhov A. P., Sukhanov M. V., Churbanov M. F., ... Kirillov Yu. P. Behavior of hydroxyl groups in quartz glass during heat treatment in the range 750–950 °C. *Inorganic Materials*. 2018;54(9): 925–930. <https://doi.org/10.1134/S0020168518090169>
18. Hruby A. Evaluation of glass-forming tendency by means of DTA. *Czechoslovak Journal of Physics*. 1972; 22(11): 1187–1193. <https://doi.org/10.1007/BF01690134>
19. Snopatin G. E., Shiryayev V. S., Plotnichenko V. G., ... Churbanov M. F. High-purity chalcogenide glasses for fiber optics. *Inorganic Materials*. 2009;45(13): 1439–1460. <https://doi.org/10.1134/S0020168509130019>
20. Tanaka K. Have we understood the optical absorption edge in chalcogenide glasses? *Journal of Non-Crystalline Solids*. 2016;431: 21–24. <https://doi.org/10.1016/j.jnoncrysol.2015.03.006>
21. Seddon A. B., Hemingway M. A. Thermal properties of chalcogenide-halide glasses in the system: Ge–S–I. *J. Thermal Analysis*. 1991;37: 2189–2203. <https://doi.org/10.1007/BF01905586>
22. Bartenev G. M. *Structure and mechanical properties of inorganic glasses**. Moscow: Stroyizdat Publ.; 1996. 216 p. (in Russ.)
23. Sen S., Mason J. K. Topological constraint theory for network glasses and glass-forming liquids: a rigid polytope approach. *Frontiers in Materials*. 2019; 6. <https://doi.org/10.3389/fmats.2019.00213>
24. Bouzid A., Pham T.-L., Chaker Z., ... Ori. G. Quantitative assessment of the structure of $\text{Ge}_{20}\text{Te}_{73-7}\text{I}$ chalcogenide glass by first-principles molecular dynamics. *Physical Review B*. 2021;103: 094204. <https://doi.org/10.1103/PhysRevB.103.094204>
25. Jovari P., Kaban I., Bureau B., ... Zajac D.A. Structure of Te-rich Te–Ge–X (X = I, Se, Ga) glasses. *Journal of Physics: Condensed Matter*. 2010;22: 404207. <https://doi.org/10.1088/0953-8984/22/40/404207>
26. Chaker Z., Ori G., Boero M., Massobrio C. First-principles study of the atomic structure of glassy $\text{Ga}_{10}\text{Ge}_{15}\text{Te}_{75-x}$. *Journal of Non-Crystalline Solids*. 2018;498: 338–344. <https://doi.org/10.1016/j.jnoncrysol.2018.03.039>
27. Salmon P. S., Liu J. The coordination environment of Ag and Cu in ternary chalcogenide glasses. *Journal of Non-Crystalline Solids*. 1996; 205–207: 172–175. [https://doi.org/10.1016/S0022-3093\(96\)00225-6](https://doi.org/10.1016/S0022-3093(96)00225-6)
28. Scholze H. *Glass nature, structure, and properties*. New York: Springer Verlag; 1991. 454 p.
29. Larmagnac J. P., Grenet J., Michon P. Glass transition temperature dependence on heating rate and on ageing for amorphous selenium films. *Journal of Non-Crystalline Solids*. 1981;45: 157–168. [https://doi.org/10.1016/0022-3093\(81\)90184-8](https://doi.org/10.1016/0022-3093(81)90184-8)
30. Moynihan C. T., Easteal A. J., Wilder J., Tucker J. Dependence of the glass transition temperature on heating and cooling rate. *The Journal of Physical Chemistry*. 1974;78(26): 2673–2677. <https://doi.org/10.1021/j100619a008>
31. Sun J., Nie Q., Wang X., ... Ma H. Structural investigation of Te-based chalcogenide glasses using Raman spectroscopy. *Infrared Physics & Technology*. 2012;55: 316–319. <https://doi.org/10.1016/j.infrared.2012.03.003>
32. Luo Y.-R. *Comprehensive handbook of chemical bond energies*. CRC Press; 2007. 1688 p. <https://doi.org/10.1201/9781420007282>
33. Velmuzhov A. P., Tyurina E. A., Sukhanov M. V., ... Shiryayev V. S.. Effect of AgI and Te/Ge ratio on the properties of glasses in the Ge–Te–AgI system. *Optical Materials*. 2026;169: 117626. <https://doi.org/10.1016/j.optmat.2025.117626>
34. Barin I. *Thermochemical data of pure substances*. Weinheim, New York: VCH; 1995. 1885 p. <https://doi.org/10.1002/9783527619825>
35. Harris C. M., Piersol A. G. *Harris' shock and vibration handbook*. McGraw-Hill; 2002. 1456 p.
36. Cohen E. R., Cvitas T., Frey F. G., ..., Thor A. J. *Units and symbols in physical chemistry*. London: Royal Society of Chemistry; 2007. 235 p.
37. Wang F., Boolchand P., Jackson K. A., Micoulaut M. Chemical alloying and light-induced collapse of intermediate phases in chalcogenide glasses. *Journal of Physics: Condensed Matter*. 2007;19: 226201. <https://doi.org/10.1088/0953-8984/19/22/226201>
38. Holomb R., Mitsa V., Johansson P. Localized states model of GeS_2 glasses based on electronic states of Ge_nS_m clusters calculated by using TD-DFT. *Journal of Optoelectronics and Advanced Materials*. 2005;7(4): 1881–1888.
39. Palaz S., Koc H., Mamedov A.M., Ozbay E. Topological insulators: electronic band structure and spectroscopy. *IOP Conference Series: Materials Science and Engineering*. 2017;175: 012004. <https://doi.org/10.1088/1757-899X/175/1/012004>
40. Dhingra A., Lipatov A., Lu H., ... Dowben P.A. Surface and dynamical properties of GeI_2 . *2D Materials*. 2022;9(2): 025001. <https://doi.org/10.1088/2053-1583/ac4715>
41. Gordienko A. B., Zhuravlev Yu. N., Poplavnoi A. S. Electronic structure of AgCl, AgBr, and AgI. *Physica Status*

Solids (b). 1991;168(1): 49–156. <https://doi.org/10.1002/pssb.2221680114>

42. Koltashev V. V., Denker B. I., Galagan B. I., ... Plotnichenko V. G. 150 mW Tb³⁺ doped chalcogenide glass fiber laser emitting at $\lambda > 5 \mu\text{m}$. *Optics & Laser Technology*. 2023;161: 109233. <https://doi.org/10.1016/j.optlastec.2023.109233>

* Translated by author of the article

Information about the authors

Elizaveta A. Tyurina, Cand. Sci. (Chem.), Researcher at the Laboratory of High-Purity Chalcogenide Glasses for Mid-IR Photonics, G. G. Devyatykh Institute of Chemistry of High-Purity Substances of the Russian Academy of Science (Nizhny Novgorod, Russian Federation).

<https://orcid.org/0000-0002-6107-9862>
tyurina.ichps@mail.ru

Aleksandr P. Velmuzhov, Cand. Sci. (Chem.), Senior Research Fellow at the Laboratory of High-Purity Chalcogenide Glasses for Mid-IR Photonics, G. G. Devyatykh Institute of Chemistry of High-Purity Substances of the Russian Academy of Science (Nizhny Novgorod, Russian Federation).

<https://orcid.org/0000-0002-8739-3868>
velmuzhov.ichps@mail.ru

Maxim V. Sukhanov, Cand. Sci. (Chem.), Senior Research Fellow at the Laboratory of High-Purity Chalcogenide Glasses for Mid-IR Photonics, G. G. Devyatykh Institute of Chemistry of High-Purity Substances of the Russian Academy of Science (Nizhny Novgorod, Russian Federation).

<https://orcid.org/0000-0003-0525-6286>
sukhanov@ihps-nnov.ru

Aleksandr D. Plekhovich, Cand. Sci. (Chem.), Senior Research Fellow at the Laboratory of High-Purity Chalcogenide Glasses for Mid-IR Photonics, G. G. Devyatykh Institute of Chemistry of High-Purity Substances of the Russian Academy of Science (Nizhny Novgorod, Russian Federation).

<https://orcid.org/0000-0002-1726-7313>
plekhovich@ihps-nnov.ru

Diana G. Fukina, PhD, Senior Research Fellow at the Laboratory of Inorganic Materials, Lobachevsky State University of Nizhny Novgorod (Nizhny Novgorod, Russian Federation).

<https://orcid.org/0000-0001-8375-6863>
dianafuk@yandex.ru

Vladimir S. Shiryaev, Dr. Sci. (Chem.), Deputy Director for Research, G. G. Devyatykh Institute of Chemistry of High-Purity Substances of the Russian Academy of Science (Nizhny Novgorod, Russian Federation).

<https://orcid.org/0000-0002-1726-7313>
shiryaev@ihps-nnov.ru

Received June 30, 2025; approved after reviewing December 4, 2025; accepted for publication December 15, 2025; published online April 01, 2026.